Injected Current Sensitivity Based Load Flow Algorithm for Multi-Phase Distribution System in the Presence of Distributed Energy Resources

Arun Suresh, *Graduate Student Member, IEEE*, Krishna Murari, *Member, IEEE*, and Sukumar Kamalasadan, *Senior Member, IEEE*

***Abstract*—This paper presents an injected current sensitivity (ICS) based multi-phase load flow (LF) methodology with minimal Jacobian computation for the three-phase unbalanced distribution system with multiple Distributed Energy Resources (DERs). In the proposed approach, first, a generalized bus admittance and Jacobian matrix have been formulated that include various distribution system components such as lines, shunt capacitors, voltage control devices such as regulators, different transformer connections, and load models. Second, DERs are modeled as a PV bus and incorporated into the proposed LF algorithm by formulating a reactive power injection-based sensitivity matrix that iteratively computes its net power injections. Unlike the traditional Jacobian matrix-based LF methods where an update of Jacobian (size and element) is required for each PV bus, this method does not require any update, hence, making it faster and more flexible to include a large number of DERs. From the various tests performed on the standard IEEE three-phase distribution network and their derivatives, it has been observed that the proposed approach is accurate, efficient, computationally less complex, and scalable.**

***Index Terms*—DERs, injected current sensitivity, multi-phase load flow, unbalanced power distribution system.**

NOMENCLATURE

α	Off nominal tap ratio of a transformer-primary side
β	Off nominal tap ratio of a transformer-secondary side
χ	Iteration count
λ	Set of PV buses
$\mathbf{I}_{i(q)}$	Imaginary part of three phase complex current injection vector into bus i
$\mathbf{I}_{i(r)}$	Real part of 3ϕ phase complex current injection vector into bus i
$\mathbf{I}_i$	Three phase complex current injection vector of bus i
$\mathbf{P}_i$	Real part of three phase complex power injection vector into bus i
$\mathbf{Q}_i$	Reactive part of three-phase complex power injection vector into bus i
$\mathbf{S}_{DG_i}$	Three phase complex power supplied by the DG associated with bus i
$\mathbf{S}_i$	3ϕ complex power injection vector of bus i
$\mathbf{S}_{L_i}$	Three phase complex load vector at bus i
$\mathbf{V}_{i(q)}$	Imaginary part of 3ϕ complex voltage vector at bus i
$\mathbf{V}_{i(r)}$	Real part of 3ϕ complex voltage vector at bus i
$\mathbf{V}_i$	Three phase complex voltage vector of bus i
$(\Delta\mathbf{I}_{\lambda_k})^{\chi}$	Additional current injections in iteration t required at bus λ_k to compensate the difference between computed voltage and specified voltage at bus λ_k
$(\Delta\mathbf{V}_{\lambda_k})^{\chi}$	Voltage mismatch at the PV bus λ_k in the beginning of iteration count χ
μ	Total number of PV bus in the distribution network
ϕ	Phase of distribution system $\phi = (a, b, c)$
σ	Alias of ϕ where $\sigma = (a, b, c)$
d_V	Per unit voltage change per step
i	Bus number $(i = 1, 2 \ldots N)$
$I^{\phi}_{i(q)}$	Imaginary part of complex current injection into phase ϕ of bus i
$I^{\phi}_{i(r)}$	Real part of complex current injection into phase ϕ of bus i
I^{ϕ}_i	Complex current injection into phase ϕ of bus i
j	Alias of i
k	Indices of set λ i.e location of PV buses in set λ
K_1–K_3	ZIP parameters for $P^{\phi}_{L_i}$ their sum is equal to 1
K_4–K_6	ZIP parameters for $Q^{\phi}_{L_i}$ their sum is equal to 1
N	Total number of buses
P^{ϕ}_i	Real part of complex power injection into phase ϕ of bus i
Q^{ϕ}_i	Reactive part of complex power injection into phase ϕ of bus i
$S^{\phi}_{DG_i}$	Complex power supplied in phase ϕ of bus i by the DG associated with bus i
S^{ϕ}_i	Complex power injection into phase ϕ of bus i
$S^{\phi}_{L_i}$	Complex load at phase ϕ of bus i

Manuscript received 15 September 2021; revised 7 December 2021 and 24 February 2022; accepted 10 April 2022. Date of publication 14 April 2022; date of current version 28 November 2022. This work was supported by the U.S. Department of Energy's Office of Energy Efficiency and Renewable Energy (EERE) under the Solar Energy Technologies Office under Award DE-EE0008774 awarded to Sukumar Kamalasadan. Paper no. TPWRD-01386-2021. *(Corresponding author: Krishna Murari.)*

The authors are with the Power, Energy, and Intelligent Systems Laboratory, Energy Production, and Infrastructure Center (EPIC), Department of Electrical Engineering, University of North Carolina at Charlotte, Charlotte, NC 28223 USA (e-mail: asuresh4@uncc.edu; kmurari@uncc.edu; skamalas@uncc.edu).

Color versions of one or more figures in this article are available at https://doi.org/10.1109/TPWRD.2022.3167621.

Digital Object Identifier 10.1109/TPWRD.2022.3167621

$V_{i(q)}^{\phi}$	Imaginary part of phase ϕ voltage of bus i
$V_{i(r)}^{\phi}$	Real part of phase ϕ voltage of bus i
V_{i}^{ϕ}	Phase ϕ voltage of bus i
y_d	Leakage admittance of transformer d
γ_t^{ϕ}	Taps of regulator t associated with phase ϕ
$\mathbb{Y}_t^{reg}$	Phase admittance matrix of regulator t
$\mathbb{Y}_{ij}^{ser}$	Phase admittance matrix corresponding to series element of line connecting bus i and j
$\mathbb{Y}_{ij}^{sh}$	Phase admittance matrix corresponding to shunt element of line connecting bus i and j
$\mathbb{Z}_{ij}$	Phase impedance matrix corresponding to series element of line connecting bus i and j
$\mathbf{F}_t$	Three phase tap matrix of regulator t

I. Introduction

LOAD flow (LF) methodologies for unbalanced power distribution system (DS) provides voltage magnitude and angles at each node, power flowing through each branch, and the total active and reactive power losses in the system [1], [2]. LF helps to determine proper settings and locations for devices such as voltage regulators and reactive power compensating devices. Conventional methods of LF such as Guass-Seidel [1], Newton-Raphson (NR) [1], [3], fast decoupled [1], that are widely used for transmission systems (TS) exhibit poor convergence behavior when applied to DS. The reasons are but are not limited to, the network topology differences (mesh vs radial), unbalanced nature of DS including untransposed lines, combinations of single and double line sections, unbalanced loads, high R/X ratio, mutual coupling effect in DS, and large number of nodes [4], [5]. The LF methodologies are becoming significant as DS is no longer passive but include a larger number of multiple single-phase and three-phase DERs.

For DS, modified first and second-order LF methods have been proposed. Some variants of power flow and optimal power flow including Newton's algorithm viz., current injection method (CIM), have gained attention recently [6]–[8], [10], [11]. A three-phase form of the current injection method (TCIM) demonstrated in [7] is numerically robust with quadratic convergence. Even though the framework is computationally efficient, TCIM does not consider different load connection types such as Delta connected loads. Also, with multiple PV buses (as becoming a norm due to high penetration of DERs), more number of off-diagonal elements in Jacobian needs iterative updates making the Jacobian computation more complex and time-consuming especially while treating a large number of control devices [8]. The authors in [12] have presented an efficient LF algorithm using the common basis of modified-augmented-nodal analysis formulation. However, in this approach DERs models have not been considered. Another method that uses a complex bus admittance matrix and equivalent current injections called Gauss Implicit methods is presented in [13]–[16]. The approach in [13]–[15] has less computational complexity and memory usage compared to Newton Raphson methods. However, the convergence of the Zbus method is dependent upon the number of PV buses in the system and the convergence rate deteriorates as the number of PV increases [13]–[15]. On the other hand, the Zbus approach presented in [16] has not considered various DERs models.

Another approach is the well known backward-forward sweep (BFS) algorithm [9], [17]–[23]. Even though precise for certain network, BFS has some computational limitations [4], [24]. For example, the branch and bus numbering schemes used in BFS to compute the branch currents and bus voltages are time-consuming. It is also difficult to include the full model of distributed system components. Moreover, the sequential computation of bus voltages increases the computation time exponentially. Matrix-based BFS methods have addressed some of the complexity associated with primitive BFS based approaches [17]–[23], [25]. For example, the bus injection to branch current matrix (BIBC), branch current to bus voltage matrix (BCBV), and direct load flow (DLF) matrix-based methods are proposed in [26], [27] to make the LF for DS more efficient yet the computational complexity (due to multiple computations) is a major concern. In [4], [5], authors have formulated the loads beyond branch matrix, load current, and branch current matrix for computing the load current and branch currents. Even though the approach is computationally efficient, transformers and regulators models are not included.

In this paper, a new injected current sensitivity-based LF method is proposed for a multi-phase unbalanced power distribution system with multiple DERs. The main features of the proposed method are as follows.

- The proposed approach work with distributed lines with one or two phases connected to Delta/Wye constant power, constant current, and constant impedance (ZIP) loads.
- Models for lines, capacitors, voltage regulators, and transformers with various connections are derived to form a generalized bus admittance matrix (Y-bus), making the LF perform at different operating conditions.
- Generalized Jacobian matrix has been formulated which embeds the features of the generalized Y-bus.
- Multiphase DERs with voltage control capability are modeled as a sensitivity-based PV bus.
- The injected current from the PV bus is included as an additional vector thus the size and elements of the Jacobian matrix are not increased due to PV bus inclusion.
- The proposed method has good convergence ability and is computationally faster for a wide range of R/X ratio variations, load variations, and system size variations.

The paper is organized as follows. Section II summarizes different models that are required for load flow analysis. Section III discusses the proposed LF and Section IV extends the approach to include DERs. Section V discusses the results and conclusions and future works are discussed in Section VI.

II. Distribution System Modeling

In the proposed approach, first, a stacked Y bus model considering, distribution lines, voltage regulators, transformers, loads, and distributed energy resources, are developed.

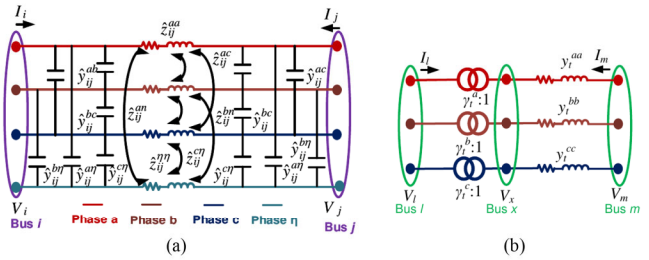

Fig. 1. Schematic representation of (a) Distribution line (b) Voltage regulator.

A. Distribution Lines

A distribution network is represented by a set of $\mathbb{K}$ buses, and a set of $\mathbb{L}$ lines connecting these buses as shown in Fig. 1(a). For a three-phase line segment connected between bus i and j with neutral, the primitive impedance [28] can be written as $\mathbb{Z}_{ij}^{prim}$. Further, this can be transformed into phase impedance matrix by suitably applying Kron's reduction, thus merging the effect of neutral conductor (η) given as $\mathbb{Z}_{ij}$

$$\mathbb{Z}_{ij}^{prim} = \begin{bmatrix} \hat{z}_{ij}^{aa} & \hat{z}_{ij}^{ab} & \hat{z}_{ij}^{ac} & \hat{z}_{ij}^{a\eta} \\ \hat{z}_{ij}^{ba} & \hat{z}_{ij}^{bb} & \hat{z}_{ij}^{bc} & \hat{z}_{ij}^{b\eta} \\ \hat{z}_{ij}^{ca} & \hat{z}_{ij}^{cb} & \hat{z}_{ij}^{cc} & \hat{z}_{ij}^{c\eta} \\ \hat{z}_{ij}^{\eta a} & \hat{z}_{ij}^{\eta b} & \hat{z}_{ij}^{\eta c} & \hat{z}_{ij}^{\eta\eta} \end{bmatrix}, \quad \mathbb{Z}_{ij} = \begin{bmatrix} z_{ij}^{aa} & z_{ij}^{ab} & z_{ij}^{ac} \\ z_{ij}^{ba} & z_{ij}^{bb} & z_{ij}^{bc} \\ z_{ij}^{ca} & z_{ij}^{cb} & z_{ij}^{cc} \end{bmatrix} \tag{1}$$

The corresponding series and shunt phase admittance will be

$$\mathbb{Y}_{ij}^{ser} = \mathbb{Z}_{ij}^{-1}, \quad \mathbb{Y}_{ij}^{sh} = \frac{1}{2}\mathbb{B}_{ij}^{sh} \tag{2}$$

where $\mathbb{B}_{ij}^{sh}$ is total three phase shunt admittance matrix of the line connecting bus i and j. The current injections at terminals i and j in complex form can then be obtained as

$$I_i = (\mathbb{Y}_{ij}^{ser} + \mathbb{Y}_{ij}^{sh})V_i - \mathbb{Y}_{ij}^{ser} f V_j \tag{3}$$

$$I_j = -\mathbb{Y}_{ij}^{ser} V_i + (\mathbb{Y}_{ij}^{ser} + \mathbb{Y}_{ij}^{sh})V_j \tag{4}$$

Therefore, the Y-bus of the distribution line connected between bus i and j is given by:

$$Y_{bus}^{dl} = \begin{bmatrix} \mathbb{Y}_{ij}^{ser} + \mathbb{Y}_{ij}^{sh} & -\mathbb{Y}_{ij}^{ser} \\ -\mathbb{Y}_{ij}^{ser} & \mathbb{Y}_{ij}^{ser} + \mathbb{Y}_{ij}^{sh} \end{bmatrix} = \begin{bmatrix} Y_{ii} & Y_{ij} \\ Y_{ji} & Y_{jj} \end{bmatrix} \tag{5}$$

B. Load Tap Changers and Voltage Regulators

Consider a voltage regulator connected between bus l and bus m as shown in Fig. 1(b). The relationship between voltage and current of the phase ϕ can be represented as

$$\frac{V_x^\phi}{V_l^\phi} = \frac{1}{\gamma_t^\phi}, \frac{I_l^\phi}{I_m^\phi} = -\gamma_\phi^s \tag{6}$$

where V_x^ϕ and V_l^ϕ are line to neutral voltages of nodes x and l respectively.

$$\gamma_t^\phi = 1 \mp \frac{T_2}{T_1} = 1 \mp \mathtt{d_V} * \mathtt{tp} \tag{7}$$

TABLE I
Y-BUS FOR VARIOUS TRANSFORMER CONNECTIONS [29]

Node n	Node 0	Ynn	Yno	Yon	Yoo
Wye-G	Wye-G	$Y_1/(\alpha)^2$	$-Y_1/(\alpha\beta)$	$-Y_1/(\alpha\beta)$	$Y_1/(\beta)^2$
Wye-G	Wye	$Y_2/(\alpha)^2$	$-Y_2/(\alpha\beta)$	$-Y_2/(\alpha\beta)$	$Y_2/(\beta)^2$
Wye	Wye-G	$Y_2/(\alpha)^2$	$-Y_2/(\alpha\beta)$	$-Y_2/(\alpha\beta)$	$Y_2/(\beta)^2$
Wye	Wye	$Y_2/(\alpha)^2$	$-Y_2/(\alpha\beta)$	$-Y_2/(\alpha\beta)$	$Y_2/(\beta)^2$
Wye-G	Delta	$Y_1/(\alpha)^2$	$Y_3/(\alpha\beta)$	${Y_3}^T/(\alpha\beta)$	$Y_2/(\beta)^2$
Wye	Delta	$Y_2/(\alpha)^2$	$Y_3/(\alpha\beta)$	${Y_3}^T/(\alpha\beta)$	$Y_2/(\beta)^2$
Delta	Delta	$Y_2/(\alpha)^2$	$-Y_2/(\alpha\beta)$	$-Y_2/(\alpha\beta)$	$Y_2/(\beta)^2$
Delta	Wye-G	$Y_2/(\alpha)^2$	$Y_3/(\alpha\beta)$	${Y_3}^T/(\alpha\beta)$	$Y_1/(\beta)^2$
Delta	Wye	$Y_2/(\alpha)^2$	$Y_3/(\alpha\beta)$	${Y_3}^T/(\alpha\beta)$	$Y_2/(\beta)^2$

where tp is the tap setting, T_1 and T_2 are number of turns of primary and secondary respectively. The current injections at bus l and m can be written as

$$I_l^\phi = \frac{y_t^{\phi\phi}}{(\gamma_t^\phi)^2} V_l^\phi - \frac{y_t^{\phi\phi}}{\gamma_t^\phi} V_m^\phi \tag{8}$$

$$I_m^\phi = -\frac{y_t^{\phi\phi}}{\gamma_t^\phi} V_s(l) + y_t^{\phi\phi} V_s(m) \tag{9}$$

Therefore, the Y-bus of a three phase voltage regulator in series with a distribution line with admittance Y_t^{reg} connected between bus l and m can be written as

$$Y_{bus}^{reg} = \begin{bmatrix} F_{\mathrm{t}} \mathbb{Y}_t^{reg} F_{\mathrm{i}}^T & F_{\mathrm{t}}(-\mathbb{Y}_t^{reg}) \\ (-\mathbb{Y}_t^{reg}) F_{\mathrm{t}}^T & \mathbb{Y}_t^{reg} \end{bmatrix} = \begin{bmatrix} Y_{ll} & Y_{lm} \\ Y_{ml} & Y_{mm} \end{bmatrix} \tag{10}$$

where

$$F_{\mathrm{t}} = \begin{bmatrix} \frac{1}{\gamma_t^a} & 0 & 0 \\ 0 & \frac{1}{\gamma_t^b} & 0 \\ 0 & 0 & \frac{1}{\gamma_t^c} \end{bmatrix}. \tag{11}$$

For the regulator control, a tap operation is initiated if the voltage at regulating point node is out of the band from a preset reference voltage. For this, an algorithm similar to the one presented in [22] is used. Then the Y bus is updated based on the new taps, and the new Jacobian is calculated.

C. Transformers

Consider a transformer connected between bus n and bus o. The Y-bus of transformer can be represented as

$$Y_{bus}^{trf} = \begin{bmatrix} Y_{nn} & Y_{no} \\ Y_{on} & Y_{oo} \end{bmatrix} \tag{12}$$

The nodal admittances of different types of transformers with leakage admittance demonstrated in [29] is shown in Table I. where

$$Y_1 = \begin{bmatrix} y_d & 0 & 0 \\ 0 & y_d & 0 \\ 0 & 0 & y_d \end{bmatrix}, Y_2 = \frac{1}{3}\begin{bmatrix} 2y_d & -y_d & -y_d \\ -y_d & 2y_d & -y_d \\ -y_d & -y_d & 2y_d \end{bmatrix} \tag{13}$$

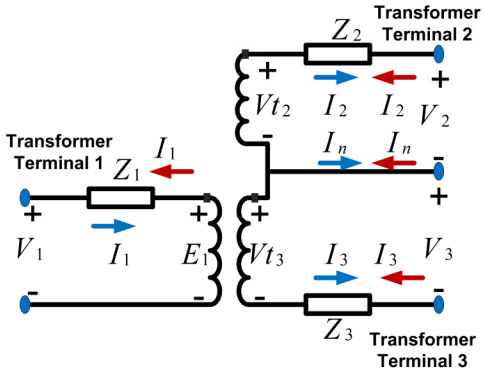

Fig. 2. Schematic representation of center-tapped transformer.

$$Y_3 = \frac{1}{\sqrt{3}} \begin{bmatrix} -y_d & y_d & 0 \\ 0 & -y_d & y_d \\ y_d & 0 & -y_d \end{bmatrix} \tag{14}$$

D. Center Tapped Transformers

The model of the single-phase center-tapped transformer is shown in Fig. 2. This transformer has three terminals (one primary and two secondary terminals). The impedances Z_1, Z_2, and Z_3 represent the individual winding impedances.

The Y-bus of centre tapped transformer can be represented as:

$$Y_{bus}^{Ctap} = \begin{bmatrix} Y_{11} & Y_{12} & Y_{13} \\ Y_{21} & Y_{22} & Y_{23} \\ Y_{31} & Y_{32} & Y_{33} \end{bmatrix} \tag{15}$$

The element of Y_{bus}^{Ctap} can be derived as follows. The ideal primary voltage E_1 as a function of the secondary terminals ideal voltages Vt_2 and Vt_3 can be represented as:

$$\begin{bmatrix} E_1 \\ E_1 \end{bmatrix} = \frac{1}{n_t} \begin{bmatrix} 1 & 0 \\ 0 & 1 \end{bmatrix} \begin{bmatrix} Vt_2 \\ Vt_3 \end{bmatrix} \tag{16}$$

where $n_t = \frac{High side rated voltage}{low side half winding rated voltage}$ The source voltage (V_1) can be written in terms of ideal primary voltage (E_1) as

$$\begin{bmatrix} V_1 \\ V_1 \end{bmatrix} = \begin{bmatrix} E_1 \\ E_1 \end{bmatrix} + \begin{bmatrix} Z_1 & 0 \\ 0 & Z_1 \end{bmatrix} \begin{bmatrix} I_1 \\ I_1 \end{bmatrix} \tag{17}$$

The ideal secondary voltages of the split phase transformer can be represented in terms of secondary terminal voltages (V_2, and V_3) as:

$$\begin{bmatrix} Vt_2 \\ Vt_3 \end{bmatrix} = \begin{bmatrix} V_2 \\ V_3 \end{bmatrix} + \begin{bmatrix} Z_2 & 0 \\ 0 & -Z_3 \end{bmatrix} \begin{bmatrix} I_2 \\ I_3 \end{bmatrix} \tag{18}$$

The primary transformer current (I_1) in terms of secondary winding currents (I_2, and I_3) can be written as:

$$\begin{bmatrix} I_1 \\ I_1 \end{bmatrix} = \frac{1}{n_t} \begin{bmatrix} 1 & -1 \\ 1 & -1 \end{bmatrix} \begin{bmatrix} I_2 \\ I_3 \end{bmatrix} \tag{19}$$

In compact form, (16), (17), (18) and (19) becomes

$$\begin{bmatrix} E_{11} \end{bmatrix} = \begin{bmatrix} av \end{bmatrix} \begin{bmatrix} Vt_{23} \end{bmatrix} \tag{20}$$

$$\begin{bmatrix} V_{11} \end{bmatrix} = \begin{bmatrix} E_{11} \end{bmatrix} + \begin{bmatrix} Z_{11} \end{bmatrix} \begin{bmatrix} I_{11} \end{bmatrix} \tag{21}$$

$$\begin{bmatrix} Vt_{23} \end{bmatrix} = \begin{bmatrix} V_{23} \end{bmatrix} + \begin{bmatrix} Z_{23} \end{bmatrix} \begin{bmatrix} I_{23} \end{bmatrix} \tag{22}$$

$$\begin{bmatrix} I_{11} \end{bmatrix} = \begin{bmatrix} ai \end{bmatrix} \begin{bmatrix} I_{23} \end{bmatrix} \tag{23}$$

Using (20) in (21), we get

$$\begin{bmatrix} V_{11} \end{bmatrix} = \begin{bmatrix} av \end{bmatrix} \begin{bmatrix} Vt_{23} \end{bmatrix} + \begin{bmatrix} Z_{11} \end{bmatrix} \begin{bmatrix} I_{11} \end{bmatrix} \tag{24}$$

Using (22) and (23) in (24), we get

$$\begin{bmatrix} V_{11} \end{bmatrix} - \begin{bmatrix} av \end{bmatrix} \begin{bmatrix} V_{23} \end{bmatrix} = \underbrace{\left[\begin{bmatrix} av \end{bmatrix} \begin{bmatrix} Z_{23} \end{bmatrix} \begin{bmatrix} ai \end{bmatrix}^{-1} + \begin{bmatrix} Z_{11} \end{bmatrix} \right]}_{[Ux]} \begin{bmatrix} I_{11} \end{bmatrix} \tag{25}$$

The current injections at bus 1 can be written as:

$$\begin{bmatrix} I_{11} \end{bmatrix} = [Ux]^{-1} \begin{bmatrix} V_{11} \end{bmatrix} + [-[Ux]^{-1}] \begin{bmatrix} av \end{bmatrix} \begin{bmatrix} V_{23} \end{bmatrix} \tag{26}$$

With this, all elements of the first row of Y_{bus}^{Ctap} matrix can be calculated. Similarly, corresponding voltages and currents related to the current injections at terminals 2 and 3 can be written as follows:

$$\begin{bmatrix} V_{11} \end{bmatrix} = \begin{bmatrix} E_{11} \end{bmatrix} - \begin{bmatrix} Z_{11} \end{bmatrix} \begin{bmatrix} I_{11} \end{bmatrix} \tag{27}$$

$$\begin{bmatrix} V_{11} \end{bmatrix} = \begin{bmatrix} av \end{bmatrix} \begin{bmatrix} Vt_{23} \end{bmatrix} - \begin{bmatrix} Z_{11} \end{bmatrix} \begin{bmatrix} I_{11} \end{bmatrix} \tag{28}$$

where

$$\begin{bmatrix} Vt_{23} \end{bmatrix} = \begin{bmatrix} V_{23} \end{bmatrix} - \begin{bmatrix} Z_{23} \end{bmatrix} \begin{bmatrix} I_{23} \end{bmatrix} \tag{29}$$

$$\begin{bmatrix} I_{11} \end{bmatrix} = \begin{bmatrix} ai \end{bmatrix} \begin{bmatrix} I_{23} \end{bmatrix} \tag{30}$$

Using (29) and (30) in (28), we get

$$\begin{bmatrix} V_{11} \end{bmatrix} - \begin{bmatrix} av \end{bmatrix} \begin{bmatrix} V_{23} \end{bmatrix} - \underbrace{\left(\begin{bmatrix} av \end{bmatrix} \begin{bmatrix} Z_{23} \end{bmatrix} + \begin{bmatrix} Z_{11} \end{bmatrix} \begin{bmatrix} ai \end{bmatrix} \right)}_{[Uy]} \begin{bmatrix} I_{23} \end{bmatrix} \tag{31}$$

The current injections at terminal 2 and 3 can be written as:

$$\begin{bmatrix} I_{23} \end{bmatrix} = [Uy]^{-1} \begin{bmatrix} av \end{bmatrix} \begin{bmatrix} V_{23} \end{bmatrix} - [Uy]^{-1} \begin{bmatrix} V_{11} \end{bmatrix} \tag{32}$$

Using (26), and (32), the Y bus matrix of centre tapped transformer can be computed and associated coefficient can be extracted with V_1, V_2 and V_3.

$$\begin{bmatrix} I_1 \\ I_2 \\ I_3 \end{bmatrix} = \begin{bmatrix} Y_{11} & Y_{12} & Y_{13} \\ Y_{21} & Y_{22} & Y_{23} \\ Y_{31} & Y_{32} & Y_{33} \end{bmatrix} \begin{bmatrix} V_1 \\ V_2 \\ V_3 \end{bmatrix} \tag{33}$$

A stacked Y_{bus} including distribution lines, regulators, and transformers is shown in Algorithm 1. This Y_{bus} approach is computationally fast. For example, in case of a reconfiguration or a tap change in the voltage regulator, only Y_{bus}^{reg} needs to be recalculated instead of recalculation full system Y_{bus}.

Algorithm 1: Stacked Y Bus Calculation.

1 Find total number of buses N and branches N_L in the distribution network.
2 Identify all types of branch components (lines, regulators and transformer) connected between two buses.
3 Get data for distribution line (RLC values), transformers (leakage impedance, type) and regulators (taps).
4 Initialize Y_{bus}, Y_{bus}^{dl}, Y_{bus}^{reg} and Y_{bus}^{trf} with a null matrix of dimension $(3N \text{x} 3N)$.
5 **for** $x = 1 : N_L$ **do**
6 **if** *branch x is "distribution line"* **then**
7 Compute Y_{bus}^{dl} using (5)
8 **end**
9 **else if** *branch x is "voltage regulator"* **then**
10 Compute Y_{bus}^{reg} using (10)
11 **end**
12 **else if** *branch x is "transformer"* **then**
13 Compute Y_{bus}^{trf} using (12)
14 **end**
15 **else if** *branch x is "Split phase or centre tapped transformer"* **then**
16 Compute Y_{bus}^{Ctap} using (26) and (32)
17 **end**
18 **end**
19 $Y_{bus} = Y_{bus}^{dl} + Y_{bus}^{reg} + Y_{bus}^{trf} + Y_{bus}^{Ctap}$

E. Load Models

The loads are modeled as ZIP loads. The load at bus i associated with phase ϕ can be modeled as

$$P_{L_i}^{\phi} = (P_{L_i}^{\phi})^0 (K_1 \left|V_i^{\phi}\right|^2 + K_2 \left|V_i^{\phi}\right| + K_3) \tag{34}$$

$$Q_{L_i}^{\phi} = (Q_{L_i}^{\phi})^0 (K_4 \left|V_i^{\phi}\right|^2 + K_5 \left|V_i^{\phi}\right| + K_6) \tag{35}$$

where $(P_{L_i}^{\phi})^0$ and $(Q_{L_i}^{\phi})^0$ are nominal values of the active power and reactive power of load associated with phase ϕ of node i respectively, and $K_1 + K_2 + K_3 = 1$, $K_4 + K_5 + K_6 = 1$.

With ZIP load modeling [2], the net specified nodal current injection can be represented as

$$(I_i^{sp})^s = -\left[\left(\frac{|S_i^s|\angle\theta^s}{|V_i^s|\angle\delta^s}\right)^* + \left(\frac{|S_i^s|}{|V_{0i}^s|}\right)\angle(\delta^s - \theta^s) + \left(\frac{V_i^s}{Z_i^s}\right)\right] \tag{36}$$

where S_i^s is scheduled power, δ is the voltage angle and θ is the power factor angle, V_{0i} is the nominal voltage, Z_i is impedance of the load. The shunt capacitance for reactive power support is modeled as a constant impedance load.

F. Modeling of Distributed Energy Resources

In the proposed approach, the DERs can be modeled as PQ bus and PV bus. The PQ model of DERs is included by treating it as a negative load. The DERs modeled as PV bus (where real power and voltage at the PV bus are specified) can be included by developing a sensitivity matrix. Using the sensitivity matrix

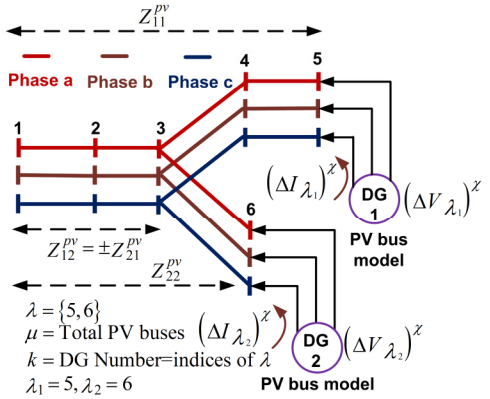

Fig. 3. Constant voltage type DGs.

net amount of reactive power is computed to compensate the difference between computed (V_{λ_k}) and specified voltage $(V_{\lambda_k^{pv}})$ at the PV bus λ_k (λ is set of PV buses and k is the indices of set λ). Consider a distribution system with total number of PV buses as μ (Fig. 3). The net complex current injections by the DERs modeled as PV bus can be computed using a generalized sensitivity matrix as

$$\mathbf{\Delta I}_{\lambda} = (\mathbf{Z^{PV}})^{-1}\mathbf{\Delta V}_{\lambda} \tag{37}$$

where $\mathbf{\Delta I}_{\lambda}$ is the additional PV bus current injection matrix to compensate for the the PV bus voltage mismatch matrix $\mathbf{\Delta V}_{\lambda}$. The matrix $\mathbf{Z^{PV}}$ is PV bus impedance matrix. where

$$\mathbf{Z^{PV}} = \begin{bmatrix} Z_{11}^{pv} & \cdots & Z_{1k}^{pv} & \cdots & Z_{1\mu}^{pv} \\ Z_{21}^{pv} & \cdots & Z_{2k}^{pv} & \cdots & Z_{2\mu}^{pv} \\ \vdots & \vdots & \vdots & \vdots & \vdots \\ Z_{\mu 1}^{pv} & \cdots & Z_{\mu k}^{pv} & \cdots & Z_{\mu\mu}^{pv} \end{bmatrix} \tag{38}$$

$$\mathbf{\Delta I}_{\lambda} = \begin{bmatrix} (\Delta I_{\lambda_1})^{\chi} & \ldots & (\Delta I_{\lambda_k})^{\chi} & \ldots & (\Delta I_{\lambda_\mu})^{\chi} \end{bmatrix}^T \tag{39}$$

$$\mathbf{\Delta V}_{\lambda} = \begin{bmatrix} (\Delta V_{\lambda_1})^{\chi} & \ldots & (\Delta V_{\lambda_k})^{\chi} & \ldots & (\Delta V_{\lambda_\mu})^{\chi} \end{bmatrix}^T \tag{40}$$

In the above equation for any PV bus k, the current variables is $(\Delta I(\lambda_k))^{\chi}$ which represents additional injection required at the PV bus λ_k to compensate the difference between computed and specified voltage. The voltage variables is $(\Delta V(\lambda_k))^{\chi}$ which represents voltage mismatch at PV bus λ_k.

$$(\Delta V_{\lambda_k})^{\chi} = \left|V_{\lambda_k^{pv}}\right| - |(V_{\lambda_k})^{\chi}| \tag{41}$$

The elements of matrix $\mathbf{Z^{PV}}$ can be computed using Algorithm 2.

Thus, we can compute net additional injection required at the PV bus using (37). $\mathbf{\Delta I}_{\lambda}$ is the net additional complex current injection vector and which can be split into real $\mathbf{\Delta I}_{\lambda}(\mathbf{r})$ and imaginary components $\mathbf{\Delta I}_{\lambda}(\mathbf{q})$. where

$$\mathbf{\Delta I}_{\lambda}(\mathbf{r}) = \left[(\Delta I_{\lambda 1(r))^{\chi}} \ldots (\Delta I_{\lambda k}(r))^{\chi} \ldots (\Delta I_{\lambda \mu}(r))^{\chi}\right]^T \tag{42}$$

Algorithm 2: $\mathbf{Z^{PV}}$ Building Algorithm.

1. Get line configuration (RLC values) data and PV bus location information.
2. Store PV bus location information in an array λ of dimension μ. For example from Fig.3, $\lambda = [5, 6]$, k is indices of λ.
3. Find the set of branches or connectivity existing in path connecting source bus to each PV bus λ_k and store the branch set in the path depiction set $W^{pv}_{\lambda_k}$
4. Initialize a null matrix $\mathbf{Z^{PV}}$ of the order $(\mu \times \mu)$.
5. **for** $m = 1 : \mu$ **do**
6. **for** $n = 1 : \mu$ **do**
7. **if** m=n **then**
8. $Z^{pv}_{mn} = \sum_{ij \in W^{pv}_{\lambda_m}} \mathbb{Z}_{ij}$
9. **end**
10. **else if** $m \neq n$ **then**
11. $Z^{pv}_{mn} = \sum_{ij \in (W^{pv}_{\lambda_m} \cap W^{pv}_{\lambda_n})} \mathbb{Z}_{ij}$
12. **end**
13. **end**
14. **end**
15. **if** *PV bus is single phase or two phases* **then**
16. Remove the rows and columns corresponding to missing phases from $\mathbf{Z^{PV}}$
17. **end**
18. Reshape the matrix to its three-phase equivalent form and ensure the resultant size of $\mathbf{Z^{PV}}$ is of the order $(3\mu \times 3\mu)$.

Algorithm 3: ΔI^{PV} Matrix Building Algorithm.

1. Compute all the elements of $\mathbf{\Delta I}_\lambda$ as per (37).
2. Store PV bus location information in an array λ of dimension μ and let k be the indices of λ.
3. Initialise a null matrix ΔI^{PV} of dimension $2N \times 1$.
4. **for** $m = 1 : N$ **do**
5. **if** $m \in \lambda$ **then**
6. $\Delta I^{PV}_{(2m-1)} = (\Delta I_{\lambda_k(q)})^\chi$ where λ_k=m
7. $\Delta I^{PV}_{(2m)} = (\Delta I_{\lambda_k(r)})^\chi$ where λ_k=m
8. **end**
9. **else if** $m \notin \lambda$ **then**
10. $\Delta I^{PV}_{(2m-1)} = \Delta I^{PV}_{(2m)} = 0$
11. **end**
12. **end**
13. Reshape the matrix ΔI^{PV} to its phase equivalent form and hence resultant size will be of the order $(6N \times 1)$

$$\mathbf{\Delta I}_\lambda(\mathbf{q}) = \left[(\Delta I_{\lambda 1(q))^\chi} \ldots (\Delta I_{\lambda k}(q))^\chi \ldots (\Delta I_{\lambda \mu}(q))^\chi\right]^T \tag{43}$$

The computed injection will be utilized for computing injected PV bus current sensitivity matrix ΔI^{PV} of the order $(2N * 1)$. This matrix reflects the characteristics of PV bus in the current injection algorithm which be included without updating elements and size of jacobian matrix. The detail regarding how the elements of ΔI^{PV} are computed is shown in Algorithm 3.

Consider a distribution system with N buses and two PV buses $\lambda_i = \mathrm{k}$ and $\lambda_j = \mathrm{p}$. The computed injection included as

$$\Delta I^{PV} = \begin{bmatrix} 0, \ldots, 0, (\Delta I_{\lambda_i(q)})^\chi, (\Delta I_{\lambda_i(r)})^\chi, 0, \ldots, 0, \\ (\Delta I_{\lambda_j(q)})^\chi, (\Delta I_{\lambda_j(r)})^\chi, 0, \ldots, 0) \end{bmatrix}^T \tag{44}$$

The additional real power injection by the DERs modeled as PV buses is zero. Hence, in (44) real part of the additional PV bus injections will be zero, Thus (44) can be modified as:

$$\Delta I^{PV} = \begin{bmatrix} 0, \ldots, 0, (\Delta I_{\lambda_i(q)})^\chi, 0, 0, \ldots, 0, \\ (\Delta I_{\lambda_j(q)})^\chi, 0, 0, \ldots, 0) \end{bmatrix}^T \tag{45}$$

III. Proposed Injected Current Sensitivity Based Load Flow

In the proposed approach the Jacobian matrix is formed from the bus admittance matrix where each element in the bus admittance matrix is replaced with 2×2 blocks in case of 1 phase system and each 3×3 matrix in the bus admittance matrix is replaced with 6×6 blocks in case of 3-phase system. The off-diagonal blocks obtained in the Jacobian are fixed over iterations and diagonal blocks are updated at every iteration based on the type of load model connected to that bus. For N bus, nodal current equation can be expressed as

$$I_{bus} = Y_{bus} V_{bus} = \sum_{i=1}^{N} \sum_{j=1}^{N} Y_{ij} V_j \tag{46}$$

where

$$I_{bus} = \left[I_1 I_2 \ldots I_N\right]^T \tag{47}$$

$$V_{bus} = \left[V_1 V_2 \ldots V_N\right]^T \tag{48}$$

are the nodal injection current vector and bus voltage vector of the network, respectively. The Y_{bus} of the N-bus system can be formulated as per Algorithm 1. From this the current injection in a phase ϕ of bus i can be computed as

$$I^\phi_i = \sum_{j \in \xi} \sum_{\varphi \in \sigma} Y^{\phi\varphi}_{ij} V^\varphi_j = I^\phi_{i(r)} + \mathbf{j} I^\phi_{i(q)} \tag{49}$$

$$V^\varphi_j = V^\varphi_{j(r)} + \mathbf{j} V^\varphi_{j(q)} \tag{50}$$

$$Y^{\phi\varphi}_{ij} = G^{\phi\varphi}_{ij} + \mathbf{j} B^{\phi\varphi}_{ij} \tag{51}$$

where, $\xi = (1, 2. \ldots N), \sigma = (a, b, c), i = (1, 2. \ldots \ldots N)$. In real and imaginary form (49) can be represented as:

$$I^\phi_{i(r)} = \sum_{j \in \xi} \sum_{\varphi \in \sigma} G^{\phi\varphi}_{ij} V^\varphi_{j(r)} - B^{\phi\varphi}_{ij} V^\varphi_{j(q)} \tag{52}$$

$$I^\phi_{i(q)} = \sum_{j \in \xi} \sum_{\varphi \in \sigma} G^{\phi\varphi}_{ij} V^\varphi_{j(q)} + B^{\phi\varphi}_{ij} V^\varphi_{j(r)} \tag{53}$$

Then the complex current mismatch in phase s of the bus i is

$$\Delta I^\phi_i = (I^\phi_i)^{spf} - (I^\phi_i)^{calc} \tag{54}$$

where $(I^\phi_i)^{calc} = \sum_{j \in \xi} \sum_{\varphi \in \sigma} Y^{\phi\varphi}_{ij} V^\varphi_j$, $(I^\phi_i)^{calc} = \sum_{j \in \xi} \sum_{\varphi \in \sigma} Y^{\phi\varphi}_{ij} V^\varphi_j$, $(P^\phi_i)^{spf} = P^\phi_{DG_i} - P^\phi_{L_i}$, $(Q^\phi_i)^{spf} = Q^\phi_{DG_i} -$

$Q^{\phi}_{L_i}$, $V^{\phi}_{i} = V^{\phi}_{i(r)} + \mathbf{j}V^{\phi}_{i(q)}$ and $(P^{\phi}_{i})^{spf}$, $P^{\phi}_{DG_i}$, $P^{\phi}_{L_i}$ is active component of scheduled, generated power and net load respectively at bus i, $(Q^{\phi}_{i})^{spf}$, $Q^{\phi}_{DG_i}$, and $Q^{\phi}_{L_i}$ is reactive component of scheduled, generated power and net load respectively at bus i. Thus (54) which is in complex form can be represented in terms of the real and imaginary component as

$$\Delta I^{\phi}_{i(r)} = \frac{(P^{\phi}_{i})^{spf}V^{\phi}_{i(r)} + (Q^{\phi}_{i})^{spf}V^{\phi}_{i(q)}}{(V^{\phi}_{i(r)})^2 + (V^{\phi}_{i(q)})^2} - \sum_{j\in\xi}\sum_{\varphi\in\sigma} G^{\phi\varphi}_{ij}V^{\varphi}_{j(r)} - B^{\phi\varphi}_{ij}V^{\varphi}_{j(q)} \tag{55}$$

$$\Delta I^{\phi}_{i(q)} = \frac{(P^{\phi}_{i})^{spf}V^{\phi}_{i(q)} - (Q^{\phi}_{i})^{spf}V^{\phi}_{i(r)}}{(V^{\phi}_{i(r)})^2 + (V^{\phi}_{i(q)})^2} - \sum_{j\in\xi}\sum_{\varphi\in\sigma} G^{\phi\varphi}_{ij}V^{\varphi}_{j(q)} + B^{\phi\varphi}_{ij}V^{\varphi}_{j(r)} \tag{56}$$

The power flow formulation using current injections considering DERs connected at bus at bus k and p can be solved using (57) as

$$\Big[\Delta V\Big] = \Big[J\Big]^{-1}\Big(\Big[\Delta I\Big] + \Big[(\Delta I^{PV}\Big]\Big) \tag{57}$$

where

$$\mathbf{J} = \begin{bmatrix}\mathbf{J_1} & \cdots & \mathbf{J_k} & \cdots & \mathbf{J_p} & \cdots & \mathbf{J_N}\end{bmatrix}^T \tag{58}$$

$$\mathbf{J_i} = \begin{bmatrix} J^{11}_i & J^{21}_i & \cdots & J^{1N}_i & J^{2N}_i \\ J^{31}_i & J^{41}_i & \cdots & J^{3N}_i & J^{4N}_i \end{bmatrix} \tag{59}$$

where $J^{1j}_i = \frac{\partial \mathbf{I}_{i(q)}}{\partial \mathbf{V}_{j(r)}}$, $J^{2j}_i = \frac{\partial \mathbf{I}_{i(q)}}{\partial \mathbf{V}_{j(q)}}$, $J^{3j}_i = \frac{\partial \mathbf{I}_{i(r)}}{\partial \mathbf{V}_{j(r)}}$ $J^{4j}_i = \frac{\partial \mathbf{I}_{i(r)}}{\partial \mathbf{V}_{j(q)}}$, and $i = \{1, 2, \ldots .N\}$ and $j = \{1, 2, \ldots .N\}$ The updated voltage is given by

$$\Big[V\Big]^{\chi+1} = \Big[V\Big]^{\chi} + \Big[\Delta V\Big] \tag{60}$$

The elements of Jacobian J can be obtained as

$$\frac{\partial I_{i(q)}}{\partial V_{j(r)}} = B_{ij} - diag(La_i),\ i = j \qquad \frac{\partial I_{i(q)}}{\partial V_{j(r)}} = B_{ij},\ i \neq j \tag{61}$$

$$\frac{\partial I_{i(q)}}{\partial V_{j(q)}} = G_{ij} - diag(Lb_i),\ i = j \qquad \frac{\partial I_{i(q)}}{\partial V_{j(q)}} = G_{ij},\ i \neq j \tag{62}$$

$$\frac{\partial I_{i(r)}}{\partial V_{j(r)}} = G_{ij} - diag(Lc_i),\ i = j \qquad \frac{\partial I_{i(r)}}{\partial V_{j(r)}} = G_{ij},\ i \neq j \tag{63}$$

$$\frac{\partial I_{i(r)}}{\partial V_{j(q)}} = -B_{ij} - diag(Ld_i),\ i = j \qquad \frac{\partial I_{i(r)}}{\partial V_{j(q)}} = -B_{ij},\ i \neq j \tag{64}$$

The elements La, Lb, Lc, Ld depends on type of load connected [7] and can be calculated as below.

$$La^{\phi}_i = \frac{K_6(Q^{\phi}_{L_i})^0(VL1) - (VL2)K_3(P^{\phi}_{L_i})^0}{(VL)^4} + \frac{(VL3)K_2(P^{\phi}_{L_i})^0 + (VL4)K_5(Q^{\phi}_{L_i})^0}{(VL)^3} + K_4(Q^{\phi}_{L_i})^0 \tag{65}$$

$$Lb^{\phi}_i = \frac{K_3(P^{\phi}_{L_i})^0(VL1) + (VL2)K_6(Q^{\phi}_{L_i})^0}{(VL)^4} - \frac{(VL3)K_5(P^{\phi}_{L_i})^0 + (VL4)K_2(P^{\phi}_{L_i})^0}{(VL)^3} - K_1(P^{\phi}_{L_i})^0 \tag{66}$$

$$Lc^{\phi}_i = \frac{K_3(P^{\phi}_{L_i})^0(VL5) - (VL2)K_6(Q^{\phi}_{L_i})^0}{(VL)^4} + \frac{(VL3)K_5(Q^{\phi}_{L_i})^0 - (VL6)K_2(P^{\phi}_{L_i})^0}{(VL)^3} - K_1(P^{\phi}_{L_i})^0 \tag{67}$$

$$Ld^{\phi}_i = \frac{K_6(Q^{\phi}_{L_i})^0(VL1) - (VL2)K_3(P^{\phi}_{L_i})^0}{(VL)^4} + \frac{(VL3)K_2(P^{\phi}_{L_i})^0 - (VL6)K_5(Q^{\phi}_{L_i})^0}{(VL)^3} - K_4(Q^{\phi}_{L_i})^0 \tag{68}$$

where VL1 $= [(V^{\phi}_{i(r)})^2 - (V^{\phi}_{i(q)})^2]$, VL2 $= 2V^{\phi}_{i(r)}V^{\phi}_{i(q)}$ VL3 $= V^{\phi}_{i(r)}V^{\phi}_{i(q)}$, VL4 $= (V^{\phi}_{i(r)})^2$, VL $= [(V^{\phi}_{i(r)})^2 + (V^{\phi}_{i(q)})^2]$ VL5 $= [(V^{\phi}_{i(q)})^2 - (V^{\phi}_{i(4)})^2]$, VL6 $= (V^{\phi}_{i(q)})^2$. For enforcing the reactive power limit, the generator's lower and upper bounds are specified. If this is violated, reactive power generation is set to the limits, and load flow is calculated treating that particular bus as a PQ bus. A flowchart of the injected current sensitivity-based load flow is shown in Fig. 4.

IV. Simulation Results and Discussions

In this section, precision, efficacy, scalability, and robustness of the proposed current injection-based LF algorithm developed on MATLAB software have been thoroughly investigated using a desktop computer with an 11th generation CORE i7 processor, 12 GB RAM, 512 GB Solid-state drives and 2.80 GHz CPU. Various test systems have been used for this purpose. A summary of the characteristics of the test systems used is shown in Table II. The precision test has been performed by comparing the test results obtained by the proposed LF algorithm with benchmark solutions [30], [31], whereas, the efficacy investigation has been conducted by comparing the convergence time of the developed LF methodology with other prevailing methodologies in the literature. The robustness of the algorithm has been analyzed by varying the R/X ratio of the distribution line data and loading

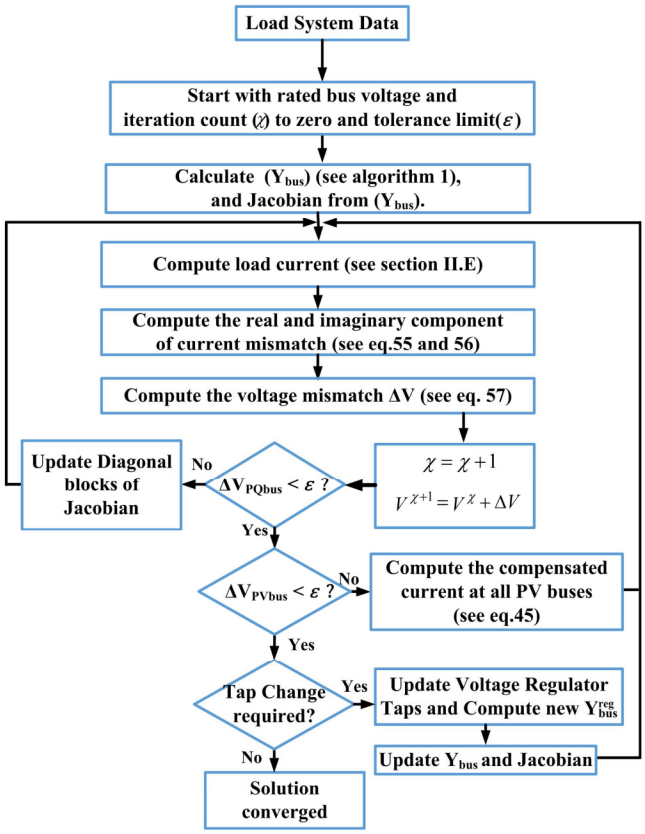

Fig. 4. Flowchart for the proposed injected current sensitivity based LF.

TABLE II
TEST SYSTEMS DESCRIPTION

Sl No	Test System	Voltage Regulators	Transformers	Shunt Caps	Avg R/X
1	IEEE 4 Bus	0	1	0	.2522
2	IEEE 13 Bus	1	1	2	0.3514
3	IEEE 123 Bus	4	1	4	0.2645
4	650 Bus	4	0	4	0.2145
5	2500 Bus	4	0	4	0.2145
5	8500 Node	4	1177	4	0.2145

factor to a very wide range. Finally, the scalability of the proposed methodology has been analyzed on three large distribution networks viz.650 bus, 2500 bus system, and IEEE 8500 node system.

A. Test System 1: IEEE-4 Bus System

The IEEE-4 bus system was used as a test system for verifying the applicability of the proposed LF algorithm for different types of transformer connections in the distribution network. Load flow analysis of transformer integrated distribution system with balanced and unbalanced loading conditions are validated with benchmark test results [30], [31] for five different transformer connections. The maximum % error in bus voltage magnitude when compared with the benchmark value for five different step-down transformer connections is shown in Fig. 5. It is evident from the test results that the LF solution obtained using

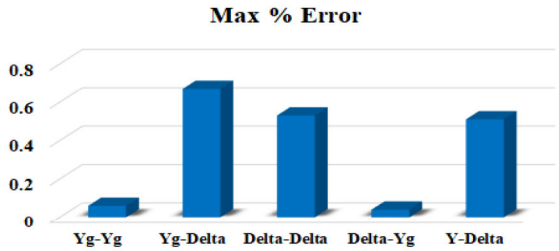

Fig. 5. Maximum % bus voltage magnitude error for different transformer connections.

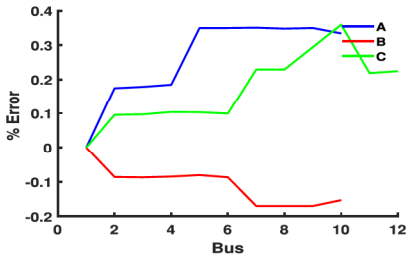

Fig. 6. Validation of LF and % error for IEEE 13 bus system.

the proposed LF methodology is within the proximity of the benchmarked test results.

B. Test Systems 2 : IEEE-13 Bus System

The IEEE-13 bus system is a heavily loaded short feeder with a substation voltage regulator and one inline transformer. This feeder is mainly used to test the effectiveness of the algorithm in handling different load types (viz. constant power (P), constant current (I), constant impedance (Z), and composite load or ZIP load), and connections of load (viz. star/delta). The load flow results obtained using the proposed current injection-based approach have been compared with benchmarks test results (Fig. 6). From this test, it is observed that the maximum percentage voltage magnitude error is within 0.4%. Thus, it can be concluded that the developed LF methodology is proficient in handling various types and connections of load. This test feeder is also used to check the ability of the proposed method on voltage regulator operations. For this, the loading is increased to 120% of the baseload yielding a lower voltage profile. A tap operation is initiated if the voltage at regulating point node is out of band from a preset reference voltage. Using the updated taps, only the $Ybus$ corresponding to regulators are calculated and system $Ybus$ is updated. The LF with new $Ybus$ and new Jacobian has performed again. The voltage profile before and after regulator tap operation is depicted in Fig. 7.

C. Test 3: IEEE-14 Bus System

A single-phase IEEE-14 bus system [6] has been used to quantitatively compare the computational efficiency of the proposed method in terms of the size of the Jacobian. The number of elements updated in Jacobian per iteration and size of Jacobian for an n bus single-phase distribution system with m PV buses

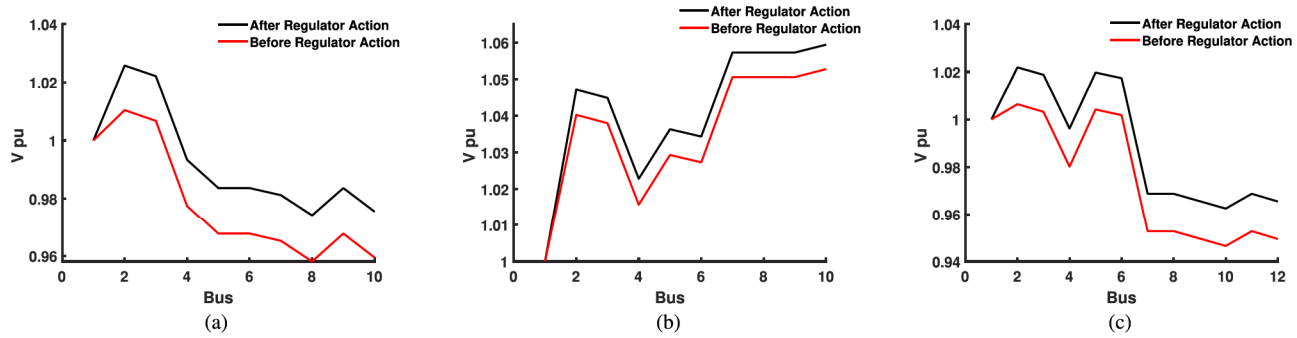

Fig. 7. Change in phase voltage with and without regulator action for IEEE 13 bus system. (a) Phase A. (b) Phase B. (c) Phase C.

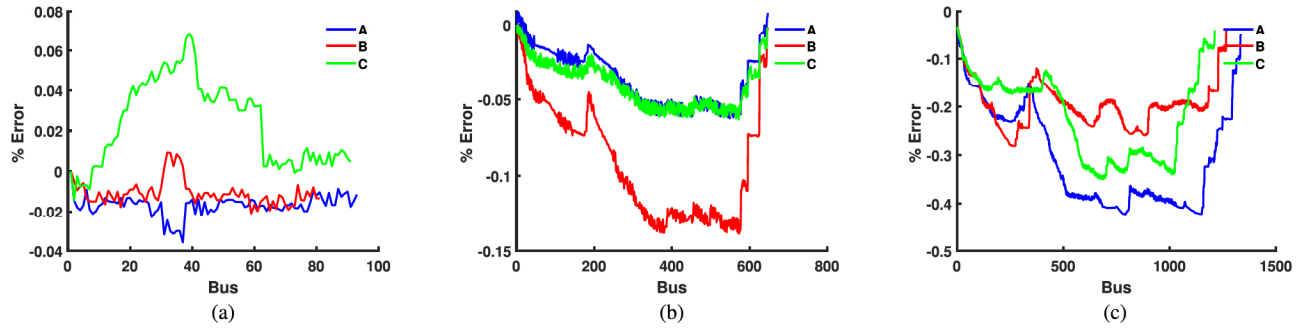

Fig. 8. Validation of LF results and % error plots for IEEE-123 bus, 650 bus and 2500 bus systems. (a) Error 123 bus. (b) Error 650 bus. (c) Error 2500 bus.

TABLE III
COMPARISONS OF JACOBIAN SIZE FOR LF APPROACHES

	Tradition NR	Current Injection [6]	Current Injection [32]	Proposed Method
Size of Jacobian	2n-m-2	2n-2	2n-2+m	2n-2
Size of Jacobian (14 bus system)	22	26	30	26
Elements Updated per Iteration	146	74	60	52

TABLE IV
COMPARISON OF THE PROPOSED APPROACH AND NR FOR VARIOUS R/X RATIOS

R/X Factor	Newton Raphson		Proposed Method	
	Iterations	Time(s)	Iterations	Time(s)
0.25	6	1.031031	5	0.0516
0.5	6	1.120756	5	0.051
1	6	1.236635	5	0.0518
2	7	1.356	5	0.051
3	9	1.897	6	0.064
5	NC	NC	8	0.078

is shown in Table III. The quantitative assessment of the size of Jacobian for the IEEE 14 bus system with 4 PV buses is depicted in Table III. Unlike the traditional Jacobian matrix-based LF methods where an update of Jacobian (size and element) is required for each PV bus, this method does not require any Jacobian update, hence, making it faster and more flexible to include a large number of DERs. The detailed validation of the convergence ability of the proposed LF method is presented next.

D. Test System 4: IEEE-123 Bus System

The IEEE-123 bus system is a heavily loaded feeder with one three phase and 6 single phase voltage regulators and four capacitors. The IEEE-123 bus system has been used to prove the applicability of the proposed LF algorithm on the system with more number of regulators. The load flow results (bus voltage magnitude) obtained using the proposed method are compared with benchmark test result. It can be seen that the solution obtained lies in the proximity of the benchmark solution (Fig. 8(a)). This elucidates the accuracy of the proposed method in the presence of number of regulators.

To prove the robustness and efficiency of the proposed LF approach, the R/X ratio and loading factor of the IEEE-123 bus distribution network have been varied. The convergence speed comparison at different loading conditions and various R/X ratios are depicted in Tables IV and V respectively. The proposed approach is much faster than the NR method due to minimal Jacobian computation per iteration. From Tables IV and V it can also be seen that the developed methodology is capable of providing the LF solution efficiently for a wide range of R/X ratios, and loading variation. This demonstrates the robustness and efficiency of the proposed LF algorithm.

To show the effectiveness of the proposed method in dealing with multiphase DERs, a test case with 1-phase (bus 151), 2-phase (bus 27), and 3-phase DERs (bus 66) in 123 bus

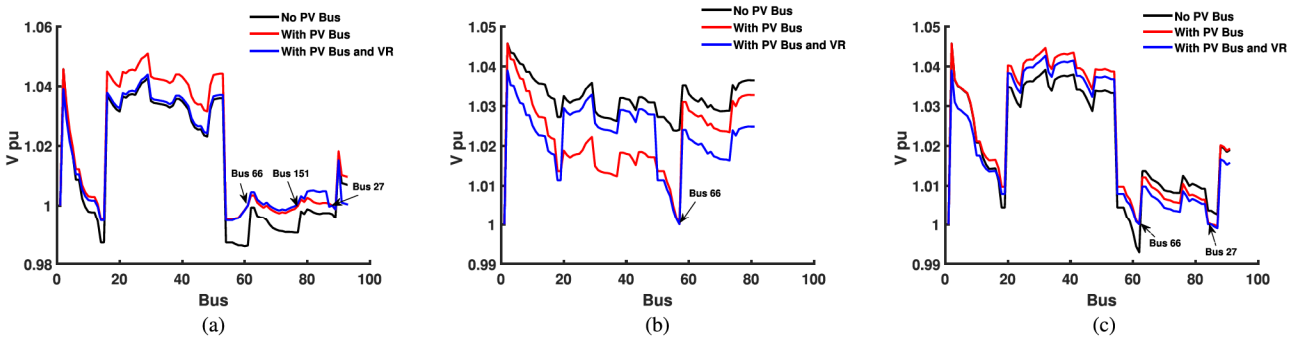

Fig. 9. Performance comparisons of proposed LF with DERs as PV Bus on IEEE-123 bus system including voltage regulators. (a) Phase A. (b) Phase B. (c) Phase C.

TABLE V
COMPARISON OF THE PROPOSED APPROACH AND NR FOR VARIOUS LOADING CONDITIONS

Loading Factor	Newton Raphson		Proposed Method	
	Iterations	Time (s)	Iterations	Time (s)
0.1	6	1.209253	6	0.0585
0.5	6	1.18596	5	0.0493
1	6	1.236635	5	0.0518
1.5	6	1.107104	5	0.0541
2	6	1.085354	6	0.0595
2.5	7	1.368683	7	0.0701
3	9	1.608643	8	0.08
4	NC	NC	19	0.1924

systems has been used. This test feeder is also used to check the ability of the proposed method on voltage regulator operations in the presence of capacitors and controlled DERs. For this, the voltage magnitude set point at all the PV buses is assumed to be maintained at 1 p.u. Three cases have been investigated. The LF results of IEEE-123 bus system without DERs (Case 1), with DERs modeled as PV bus but with no regulator control operation (Case 2), and with DERs modeled as PV bus integrated with regulator control operation (Case 3) are provided in Fig. 9. The voltage profile before and after regulator tap operation is also shown in Fig. 9. The load flow result showing location and reactive power injection per phase for all the above-mentioned scenarios is summarized in Tables VI and VII. In the third case, a tap operation is initiated if the voltage at regulating point node is out of the band from a preset reference voltage. Using the updated taps computed using the algorithm mentioned in [22], only the $Ybus$ corresponding to regulators are calculated and system $Ybus$ is updated. The LF with new $Ybus$ and new Jacobian has performed again. It has been observed that the LF results in the presence of regulators, capacitors, and DERs converging and provides a coordinated solution.

E. Test Systems 5, 6 and 7: 650 Bus System, 2500 Bus System, and 8500 Bus System

To assess the effect of the system size on the convergence and accuracy of the proposed LF model, the LF problem of three test feeders (650 bus system, 2500 bus system, and 8500 bus system) was solved using the proposed model. The 8500-node test feeder consists of multiple feeder regulators, capacitor banks, split-phase service transformers, and feeder secondaries. The circuit has a 115 kV source, 12.47 kV medium voltage feeder sections, and a 120 V low voltage feeder section. There are 4876 three-phase, two-phase, and single-phase medium-voltage nodes. The single-phase nodes are connected to 1177 split phase transformers. The two secondaries of these transformers are connected to load nodes using triplex lines. In total, there are 3041 A phase nodes, 2830B phase nodes, and 2660C phase nodes. The 650 bus system and 2500 bus system have been derived from the 8500 test system. The details about the components of the 650 bus system and 2500 bus system are provided in Table II. The load flow solution is obtained for the aforementioned scaled test systems using the proposed approach and has been compared with benchmarks test results. The deviation of voltage magnitude obtained using the proposed method when compared to OpenDSS [31] for 650 bus system and 2500 bus system are shown in Fig. 8(b) and 8(c) respectively. It can be observed that the $\%$ error deviations are less than 0.4 max that has been observed on 2500 node system. The voltage magnitude for the IEEE-8500 bus system is shown in Fig. 10. It was observed that the voltage profile is similar to the benchmark from OpenDSS. For error comparisons, maximum $\%$ error, minimum percentage error, and average percentage error in voltage deviations for the IEEE-8500 test system are provided in Table VIII. The maximum $\%$ error on the low voltage and high voltage feeders of the IEEE-8500 bus system are -0.48% and -0.41% respectively. It is evident from the error comparison plots (Fig. 8(b)–8(c)) and Table VIII that results are within 0.5 $\%$ maximum error and the error trend is not increasing considering the system scale. Test results for the assessment of DERs as PV bus are illustrated in Table IX. It can be seen that the proposed approach is capable of providing load flow solutions, accurate, and at the same time capable of coordinating legacy and DER controllable devices. The load flow solution for the IEEE-8500 node system converges in 51 s. The existing load flow reported in the literature takes more than 1500 s [33], and 150 s [34] respectively. This illustrates the efficacy and scalability of the proposed approach for large test networks. The computational time can be further improved by efficient coding and compiling procedures.

TABLE VI
SUMMARY OF LF RESULTS WITH AND WITHOUT DER CONTROL AS PV BUS FOR IEEE-123 BUS SYSTEM

Bus	No PV Bus						With PV Bus					
	Voltage(pu)			Active Power(KW)			Voltage(pu)			Reactive power injection(Kvar)		
	Ph. a	Ph. b	Ph. c	Ph. a	Ph. b	Ph. c	Ph. a	Ph. b	Ph. c	Ph. a	Ph. b	Ph. c
151	0.9884			20			0.9998			49.57		
27	0.9952		1.0027	30		25	0.9999		0.9999	-27.72		-57.86
66	0.9850	1.0250	0.9924	20	10	15	0.9999	1.0003	0.9991	73.38	-65.93	38.43

TABLE VII
SUMMARY OF LF RESULTS WITH AND WITHOUT DER CONTROL AS PV BUS AND REGULATOR CONTROL FOR IEEE-123 BUS SYSTEM

Bus	With PV Bus and No Voltage Regulator Control						With PV Bus and Voltage Regulator Control					
	Voltage(pu)			Reactive power injection(Kvar)			Voltage(pu)			Reactive power injection(Kvar)		
	Ph. a	Ph. b	Ph. c	Ph. a	Ph. b	Ph. c	Ph. a	Ph. b	Ph. c	Ph. a	Ph. b	Ph. c
151	0.99			49.5			0.99			47.8		
27	0.99		0.99	-27.7		-57.86	0.99		0.99	82.8		21.9
66	0.99	1.00	0.99	73.3	-65.9	38.43	0.99	1.00	0.99	125.6	16.5	91.3

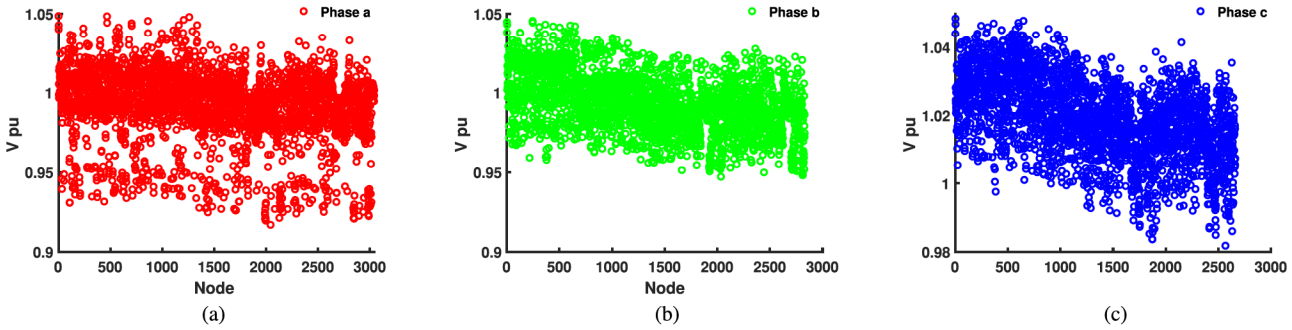

Fig. 10. IEEE 8500 node system voltage profile. (a) Phase A. (b) Phase B. (c) Phase C.

TABLE VIII
VOLTAGE MAGNITUDE % ERROR COMPARISON FOR IEEE-8500 BUS SYSTEM

% Error	High Voltage Feeder Side	Low Voltage Feeder Side	Overall System
Maximum	-0.41	-0.48	-0.48
Minimum	-0.01	-0.14	-0.14
Average	-0.24	-0.31	-0.2706

F. Discussions

The various test system has been performed to investigate the significance of the proposed current injections-based LF algorithm with the DER model and coordination with legacy devices. The first test system is the IEEE-4 bus system which has been utilized to analyze the applicability and accuracy of the developed LF methodology for transformer integrated distribution system. The test results in Fig. 5 reveal that the maximum % error from benchmark values in voltage magnitude for a step-down transformer with various connections is less than 0.8%. This has been possible because of the detailed model of different transformer connections that can be accurately included in the generalized Y-bus of the network. The second test system is the IEEE-13 bus system. The maximum % error from benchmark values in voltage magnitude is less than the 0.4% (Fig. 6) which proves that LF is accurate and also can handle regulator, transformer, and load types (viz. constant power (P), constant current (I), constant impedance (Z) and composite load) and connections of load (viz. star/delta). This can be attributed to the capability of the generalized stacked Y-bus framework.

It is evident from Tables IV and V that the proposed approach is much faster than the NR method since only diagonal blocks are updated in Jacobian per iteration in the proposed method. Also with the inclusion of the PV bus, the number of Jacobian elements updated per iteration remain unchanged. The effectiveness of multi-phase DER modeling is depicted in Table VI where the load flow results showing location and reactive power injection per phase are summarized. Table VII summarized the capability of the proposed algorithm to provide a coordinated solution considering the operation of the legacy devices and DERs. To test the scalability of the proposed method, three test feeders viz. 650 buses, 2500 buses, and 8500 buses have been considered. It is evident from the error comparison plots (Fig. 8(b)–8(c)) and Table VIII that the results are within the proximity of the benchmarked test solutions. This proves the scalability of the proposed load flow approach. Table IX summarizes the capability of the proposed method to provide

TABLE IX
SUMMARY OF THE PROPOSED LF RESULTS WITH AND WITHOUT DER CONTROL AS PV BUS FOR IEEE-8500 NODE SYSTEM

Bus	No PV Bus						With PV Bus					
	Voltage(pu)			Active Power(KW)			Voltage(pu)			Reactive power injection(Kvar)		
	Ph. a	Ph. b	Ph. c	Ph. a	Ph. b	Ph. c	Ph. a	Ph. b	Ph. c	Ph. a	Ph. b	Ph. c
L3216348	0.991	-	-	120	-	-	1.005	-	-	145	-	-
M1027005	-	0.992	-	-	150	-	-	1.005	-	-	105	-
N1140516	-	-	1.01	-	-	100	-	-	1.005	-	-	-85

TABLE X
COMPARISON OF THE PROPOSED LF WITH OTHER STATE-OF-THE-ART LF APPROACHES

LF Method	PV Bus Model	Detailed Y-Bus	Jacobian Calculated	Unbalanced/ loads	Transformer Types	Regulators	Load Types	Load Connection	IEEE Test Systems
Proposed	Yes	Yes	Yes	Yes	Yes	Yes	ZIP	Y,D	4,13,34,123,8500
[7]	Yes	No	Yes	Yes	No	No	ZIP	Y	None
[33]	No	Yes	Yes	Yes	Yes	Yes	ZIP	Y,D	37,123,8500
[4]	Yes	NA	NA	Yes	No	No	ZIP	Y	13,37,123
[26]	No	NA	NA	Yes	No	No	PQ	Y	37
[15]	No	Yes	NA	Yes	Yes	No	PQ	Y,D	None

optimal DER operation settings on a scaled system. In Table X, a comparison of the proposed LF method with the several existing LF approaches in terms of inclusion of various distribution system components has been detailed. It is evident from the test result that, the proposed LF algorithm is capable of providing the LF solution for distribution systems embedded with unbalanced loads, regulators, various load types, star and delta configuration of load, and PV type DERs.

V. CONCLUSION AND FUTURE WORK

An injected current sensitivity (ICS) for distribution systems with multi-phase DERs has been proposed. The significance of the proposed LF methodology lies in the formulation of the generalized Y-bus and Jacobian model which embeds models of all the significant components of the distribution network. This includes distribution lines, capacitors, voltage regulators, and relevant transformer connections, and a stacked bus admittance matrix (Y-bus) is designed. Then a generalized Jacobian matrix is developed. Multiphase DERs with voltage control capability are modeled as PV buses using a reactive power sensitivity-based approach and additional injection is suitably updated in the current injection vector making the size and elements of Jacobian unchanged. Comprehensive numerical tests on IEEE-4, IEEE-13, and IEEE-123 bus test distribution systems show the accuracy and robustness of the proposed approach in handling distributed lines with missing phases, several voltage regulators, and transformer connections. The approach shows reduced computational burden when compared to other methods and shows good convergence ability for a wide range of R/X ratio variations, and load variations. The scalability of the approach is validated on variants of the IEEE- 8500 bus system. The results elucidate the viability and authenticity of the proposed method.

Future work includes adding features such as open-Y and open-Δ transformer connections and delta-connected regulators. Also, to improve the computational time advanced coding methodology and parallel computing algorithms will be explored. Further, the proposed load flow algorithm will be expanded to include micro-grid, AC-DC distribution network, and integrated transmission and distribution systems.

REFERENCES

[1] H. Saadat, *Power System Analysis*. New York, NY, USA: WCB/McGraw-Hill, 1999.

[2] W. Kersting, *Distribution System Modeling and Analysis*. Boca Raton, FL, USA: CRC Press, 2018.

[3] W. F. Tinney and C. E. Hart, "Power flow solution by Newton's method," *IEEE Trans. Power App. Syst.*, vol. PAS-86, no. 11, pp. 1449–1460, Nov. 1967.

[4] K. Murari, "Graph-theoretic based approach for the load-flow solution of three-phase distribution network in the presence of distributed generations," *IET Gener. Transmiss. Distrib.*, vol. 14, pp. 1627–1640, May 2020.

[5] K. Murari and N. P. Padhy, "A network-topology-based approach for the load-flow solution of AC-DC distribution system with distributed generations," *IEEE Trans. Ind. Informat.*, vol. 15, no. 3, pp. 1508–1520, Mar. 2019.

[6] V. M. da Costa, N. Martins, and J. L. R. Pereira, "Developments in the Newton Raphson power flow formulation based on current injections," *IEEE Trans. Power Syst.*, vol. 14, no. 4, pp. 1320–1326, Nov. 1999.

[7] P. A. N. Gara, J. L. R. Pereira, S. Carneiro, V. M. da Costa, and N. Martins, "Three-phase power flow calculations using the current injection method," *IEEE Trans. Power Syst.*, vol. 15, no. 2, pp. 508–514, May 2000.

[8] P. A. N. Gara, J. L. R. Pereira, and S. Carneiro, "Voltage control devices models for distribution power flow analysis," *IEEE Trans. Power Syst.*, vol. 16, no. 4, pp. 586–594, Nov. 2001.

[9] K. Murari and S. Kamalasadan, "Graph based power flow approach for single phase distribution system with distributed generators (DGs) considering all load types," in *Proc. IEEE Ind. Appl. Soc. Annu. Meeting*, 2021, pp. 1–8.

[10] S. Moghadasi and S. Kamalasadan, "Optimal fast control and scheduling of power distribution system using integrated receding horizon control and convex conic programming," *IEEE Trans. Ind. Appl.*, vol. 52, no. 3, pp. 2596–2606, May/Jun. 2016.

[11] A. Suresh, S. Kamalasadan, and S. Paudyal, "A novel three-phase transmission and unbalance distribution co-simulation power flow model for long term voltage stability margin assessment," in *Proc. IEEE Power Energy Soc. Gen. Meeting*, 2021, pp. 1–5.

[12] I. Kocar, J. Mahseredjian, U. Karaagac, G. Soykan, and O. Saad, "Multiphase load-flow solution for large-scale distribution systems using MANA," *IEEE Trans. Power Del.*, vol. 29, no. 2, pp. 908–915, Apr. 2014.
[13] T.-H. Chen, M.-S. Chen, K.-J. Hwang, P. Kotas, and E. A. Chebli, "Distribution system power flow analysis-a rigid approach," *IEEE Trans. Power Del.*, vol. 6, no. 3, pp. 1146–1152, Jul. 1991.
[14] J.-H. Teng, "A modified Gauss-Seidel algorithm of three-phase power flow analysis in distribution networks," *Int. J. Elect. Power Energy Syst.*, vol. 24, no. 2, pp. 97–102, 2002.
[15] J. C. M. Vieira, W. Freitas, and A. Morelato, "Phase-decoupled method for three-phase power-flow analysis of unbalanced distribution systems," *IEE Proc. Gener. Transmiss. Distrib.*, vol. 151, no. 5, pp. 568–574, 2004.
[16] M. Bazrafshan and N. Gatsis, "Convergence of the Z-bus method for three-phase distribution load-flow with ZIP loads," *IEEE Trans. Power Syst.*, vol. 33, no. 1, pp. 153–165, Jan. 2018.
[17] S. Khushalani, J. M. Solanki, and N. N. Schulz, "Development of three-phase unbalanced power flow using PV and PQ models for distributed generation and study of the impact of DG models," *IEEE Trans. Power Syst.*, vol. 22, no. 3, pp. 1019–1025, Aug. 2007.
[18] K. Mahmoud and N. Yorino, "Robust quadratic-based BFS power flow method for multi-phase distribution systems," *IET Gener. Transmiss. Distrib.*, vol. 10, no. 9, pp. 2240–2250, 2016.
[19] X. Wang, M. Shahidehpour, C. Jiang, W. Tian, Z. Li, and Y. Yao, "Three-phase distribution power flow calculation for loop-based microgrids," *IEEE Trans. Power Syst.*, vol. 33, no. 4, pp. 3955–3967, Jul. 2018.
[20] R. Verma and V. Sarkar, "Active distribution network load flow analysis through non-repetitive FBS iterations with integrated DG and transformer modelling," *IET Gener. Transmiss. Distrib.*, vol. 13, no. 4, pp. 478–484, 2019.
[21] T. Alinjak, I. Pavić, and M. Stojkov, "Improvement of backward/forward sweep power flow method by using modified breadth-first search strategy," *IET Gener. Transmiss. Distrib.*, vol. 11, no. 1, pp. 102–109, 2017.
[22] J. A. D. Massignan, B. R. Pereira, and J. B. A. London, "Load flow calculation with voltage regulators bidirectional mode and distributed generation," *IEEE Trans. Power Syst.*, vol. 32, no. 2, pp. 1576–1577, Mar. 2017.
[23] Y. Kongjeen, K. Bhumkittipich, N. Mithulananthan, I. Amiri, and P. Yupapin, "A modified backward and forward sweep method for microgrid load flow analysis under different electric vehicle load mathematical models," *Electric Power Syst. Res.*, vol. 168, pp. 46–54, 2019.
[24] U. Ghatak and V. Mukherjee, "An improved load flow technique based on load current injection for modern distribution system," *Int. J. Elect. Power Energy Syst.*, vol. 84, pp. 168–181, 2017.
[25] Y. Ju, W. Wu, B. Zhang, and H. Sun, "An extension of FBS three-phase power flow for handling PV nodes in active distribution networks," *IEEE Trans. Smart Grid*, vol. 5, no. 4, pp. 1547–1555, Jul. 2014.
[26] J.-H. Teng, "A direct approach for distribution system load flow solutions," *IEEE Trans. Power Del.*, vol. 18, no. 3, pp. 882–887, Jul. 2003.
[27] J.-H. Teng, "Modelling distributed generations in three-phase distribution load flow," *IET Gener. Transmiss. Distrib.*, vol. 2, pp. 330–340, May 2008. [Online]. Available: https://digital-library.theiet.org/content/journals/10.1049/iet-gtd_20070165
[28] W. H. Kersting and W. H. Phillips, "Distribution feeder line models," *IEEE Trans. Ind. Appl.*, vol. 31, no. 4, pp. 715–720, Jul./Aug. 1995.
[29] T.-H. Chen, M.-S. Chen, T. Inoue, P. Kotas, and E. A. Chebli, "Three-phase cogenerator and transformer models for distribution system analysis," *IEEE Trans. Power Del.*, vol. 6, no. 4, pp. 1671–1681, Oct. 1991.
[30] IEEE, "Distribution test feeders," 2017. [Online]. Available: https://site.ieee.org/pes-testfeeders/
[31] EPRI, "The open distribution system simulatortm, OpenDSS version 7.6.5," 2017. [Online]. Available: https://sourceforge.net/projects/electricdss/
[32] P. A. N. Gara, J. L. R. Pereira, S. Carneiro, M. P. Vinagre, and F. V. Gomes, "Improvements in the representation of PV buses on three-phase distribution power flow," *IEEE Trans. Power Del.*, vol. 19, no. 2, pp. 894–896, Apr. 2004.
[33] M. Bazrafshan and N. Gatsis, "Comprehensive modeling of three-phase distribution systems via the bus admittance matrix," *IEEE Trans. Power Syst.*, vol. 33, no. 2, pp. 2015–2029, Mar. 2018.
[34] E. E. Pompodakis, G. C. Kryonidis, and M. C. Alexiadis, "A comprehensive three-phase step voltage regulator model with efficient implementation in the Z-bus power flow," *Electric Power Syst. Res.*, vol. 199, 2021, Art. no. 107443. [Online]. Available: https://www.sciencedirect.com/science/article/pii/S0378779621004247

Arun Suresh (Graduate Student Member, IEEE) received the B.Tech. degree in electrical engineering from Mahatma Gandhi University, India, in 2012, the M.Tech. degree in electrical engineering from Kerala University, Thiruvananthapuram, India, in 2015, and the Ph.D. degree in electrical engineering from the University of North Carolina, Charlotte, NC, USA, in 2021. He is currently a Technical Consultant with Hitachi Energy, Raleigh, NC, USA. His research interests include power system stability and control, smart grid, and integration of renewable energy in power systems.

Krishna Murari (Member, IEEE) received the B.Tech. degree in electrical engineering from WBUT, Kolkata, India, in 2010, the M.E. degree in power systems from Thapar University, Patiala, India, in 2014, and the Ph.D. degree in electrical engineering from the Indian Institute of Technology Roorkee, Roorkee, India, in 2019. He is currently a Postdoctoral Fellow with the University of North Carolina at Charlotte, Charlotte, NC, USA, on the project ReDis-PV funded by the U.S. Department of Energy. He is a reviewer in journals, such as IEEE, IET, MDPI, and *Taylor Francis Journal*. His research interests include power system analysis, power flow studies, demand-side management, distributed control algorithms, optimal power flow, distribution network pricing, and smart grid.

Sukumar Kamalasadan (Senior Member, IEEE) received the B.Tech. degree in electrical and electronics engineering from the University of Calicut, Malappuram, India, in 1991, the M.Eng. degree in electrical power systems management from the Asian Institute of Technology, Bangkok, Thailand, in 1999, and the Ph.D. degree in electrical engineering from The University of Toledo, Toledo, OH, USA, in 2004. He is currently a Professor with the Department of Electrical and Computer Engineering, University of North Carolina at Charlotte, Charlotte, NC, USA. His research interests include intelligent and autonomous control, power systems dynamics, stability and control, smart grid, microgrid, and real-time optimization and control of power systems. Dr. Kamalasadan was the recipient of several awards, including the NSF CAREER Award and IEEE Best Paper Award.